Acta Mech 228:2363–2375 (2017)
DOI 10.1007/s00707-017-1835-2

ORIGINAL PAPER

Ning Jia · Yin Yao · Yazheng Yang · Shaohua Chen

Size effect in the bending of a Timoshenko nanobeam

Received: 27 September 2016 / Revised: 4 March 2017 / Published online: 28 March 2017

Abstract The size effect should be considered due to the large ratio of surface area to volume when the characteristic length of a beam lies in the nanoscale. The size effect in the bending of a Timoshenko nanobeam is investigated in this paper based on a recently developed elastic theory for nanomaterials, in which only the bulk surface energy density and the surface relaxation parameter are involved as independent parameters to characterize the surface property of nanomaterials. In contrast to the Euler nanobeams and the classical Timoshenko beam, not only the size effect but also the shear deformation effect in Timoshenko nanobeams is included. Closed-form solutions of the deflection and the effective elastic modulus for both a fixed–fixed Timoshenko nanobeam and a cantilevered one are achieved. Comparing to the classical solution of Timoshenko beams, the size effect is obviously significant in Timoshenko nanobeams. The shear deformation effect in nanobeams cannot be neglected in contrast to the solution of Euler–Bernoulli nanobeams when the aspect ratio of a nanobeam is relatively small. Furthermore, the size effect exhibits different influences on the bending behavior of nanobeams with different boundary conditions. A nanobeam with a fixed–fixed boundary would be stiffened, while a cantilevered one is softened by the size effect, compared to the classical solution. All the findings are consistent with the existing experimental measurement. The results in this paper should be very useful for the precision design of nanobeam-based devices.

1 Introduction

It is well known that the classical beam theory includes Euler–Bernoulli and Timoshenko solutions, respectively. The difference lies in the shear deformation effect considered in Timoshenko beams due to the relatively small aspect ratio and neglected in Euler–Bernoulli beams. Both classical beam theories were established for beams with macroscopic length scales. With the development of nanoscience and nanotechnology, a nanobeam is adopted in many precise instruments. For example, nanobeams (nanowires) have found their potential applications as one of the basic building blocks in flexible electronics [1], biological sensors [2], nano-electro-mechanical systems (NEMS) [3], and reinforcing phases in advanced nanocomposites [4]. How to predict accurately the mechanical behavior of nanobeams should be very important for the precise measurement in nanoscales.

The static bending experiment has been widely used in order to investigate the bending behavior of nanobeams. It was interestingly found that nanobeams possess size-dependent mechanical properties in contrast to beams with macroscopic scales. Such a phenomenon is usually called size effect or surface effect of

N. Jia
LNM, Institute of Mechanics, Chinese Academy of Sciences, Beijing 100190, China

Y. Yao · Y. Yang · S. Chen (✉)
Institute of Advanced Structure Technology and Beijing Key Laboratory of Lightweight Multi-functional Composite Materials and Structures, Beijing Institute of Technology, Beijing 100081, China
E-mail: chenshaohua72@hotmail.com; shchen@bit.edu.cn

nanomaterials, which is due to the large surface-to-volume ratio of nanomaterials [5]. Besides of the size effect in nanobeams in contrast to macro-beams, the bending behavior of a nanobeam itself is also affected by the boundary condition. The effective Young's modulus of a nanobeam with a fixed–fixed boundary shows an opposite size-dependent behavior to that of a cantilevered nanobeam. That is, the former increases while the latter decreases with a reducing characteristic size [6–12]. It is very obvious that such interestingly experimental phenomena in nanoscale cannot be predicted by the classical beam model. A proper theory considering the size effect (surface effect) in nanomaterials should be required.

Fortunately, several theoretical models have been well established for nanomaterials within the framework of surface elasticity theory [13,14], for example, Dingreville et al. [15] formulated a framework by incorporating the surface free energy into the continuum theory of mechanics to demonstrate the size-dependent overall elastic behavior of structural elements. Duan et al. [16] extended the surface elasticity theory to nano-inhomogeneities taking into account the surface/interface stress effect. The size effect of nanobeams has also been well investigated based on the above-improved surface elasticity theory [17–22], in which the predicted effective elastic modulus depending on the characteristic size of nanobeams is consistent with the existing experimental data and molecular dynamics (MD) results [19,23–25].

In most of the above theoretical models, nanobeams were treated as the Euler–Bernoulli case without considering the shear deformation effect, which should be reasonable for a slender nanobeam with the aspect ratio larger than 10. If the aspect ratio of a nanobeam is less than 10, i.e., a stubby one, the shear deformation effect cannot be neglected, and a Timoshenko beam model is more appropriate to predict the bending behaviors [26–28]. The prediction shows a smaller effective elastic modulus for a Timoshenko nanobeam than that for an Euler–Bernoulli one, which demonstrates that shear deformation could induce softening of a nanobeam.

In the existing theoretical analyses for both Euler–Bernoulli and Timoshenko nanobeams, surface elastic constants, including surface elastic modulus and surface bending modulus, are required to serve as important parameters to characterize the surface effect in nanobeams. Till now, the surface elastic constants can hardly be measured by experiment, and the adopted values of surface elastic constants in existing theoretical literatures are almost provided by MD simulations [19,29–31]. However, to determine surface elastic constants is still a cumbersome and painstaking job, which may be inevitably affected by several numerical factors, such as how to choose a proper atomic potential, how to choose the numerical model size, and how many atom layers could be regarded as the surface of a nanobeam. Furthermore, theoretical analysis found that the stiffening and softening behavior of nanobeams is closely related to the sign of surface elastic constants and surface residual stress [17–19]. Therefore, how to determine surface elastic constants in the classical surface elasticity theory is a key problem, which is worth focusing in the future.

Recently, a new elastic theory has been developed for nanomaterials by Chen and Yao [32], in which only the surface energy density of bulk materials and the surface relaxation parameter of nanomaterials are involved. The surface elastic constant in the classical surface elasticity theory is no longer involved. Both the surface energy density of bulk materials and the surface relaxation parameter are easy to determine with clearly physical meanings. Such a new theory has been used to analyze the static bending, resonant vibration, and buckling of Euler–Bernoulli nanobeams, the results of which agree well with existing experimental measurements [33–35].

Considering the shear deformation, we further apply the new elastic theory to a Timoshenko nanobeam in this paper. Closed-form solutions of the bending deflection and the effective elastic modulus of nanobeams are achieved, which will be used to compare with the prediction of an Euler–Bernoulli nanobeam and the classical solution of a Timoshenko beam. The stiffening and softening mechanisms of nanobeams in contrast to classical beams will be further analyzed.

2 Brief introduction of the new theory for nanomaterials

The elastic theory developed by Chen and Yao [32] is based on the surface energy density of nanomaterials, which can be further expressed by the surface energy density of corresponding bulk materials and the surface relaxation parameter. Similar to the existing surface elastic models [36], the equilibrium equation and boundary conditions can be written as

$$\begin{cases} \boldsymbol{\sigma} \cdot \nabla + \boldsymbol{f} = 0 \,(\text{in} V - S) \\ \boldsymbol{n} \cdot \boldsymbol{\sigma} \cdot \boldsymbol{n} = \boldsymbol{p} \cdot \boldsymbol{n} - \gamma_n \boldsymbol{n} \,(\text{on} S) \\ (\boldsymbol{I} - \boldsymbol{n} \otimes \boldsymbol{n}) \cdot \boldsymbol{\sigma} \cdot \boldsymbol{n} = (\boldsymbol{I} - \boldsymbol{n} \otimes \boldsymbol{n}) \cdot \boldsymbol{p} - \boldsymbol{\gamma}_t \,(\text{on } S) \end{cases} \tag{1}$$

where $\boldsymbol{\sigma}$ is the bulk Cauchy stress tensor, and ∇ is a gradient operator. $\boldsymbol{n}$ is the unit normal vector perpendicular to the boundary surface S of a nano-solid; $\boldsymbol{I}$ is a unit tensor; $\boldsymbol{f}$ and $\boldsymbol{p}$ are the body force and external surface

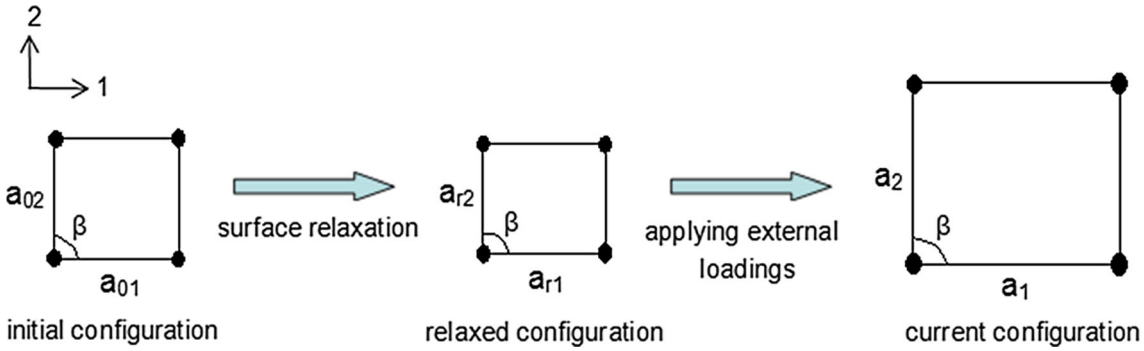

Fig. 1 Schematic of a surface unit cell in the initial (reference), relaxed, and current configurations, where the lattice lengths will change with the relaxation behavior and the external load

traction, respectively. γ_n and $\boldsymbol{\gamma}_t$ are the normal and tangential components of an additional surface-induced traction vector, respectively, which characterizes the force disturbance at boundaries due to the surface effects. V is the volume of a nano-solid, and S denotes the surface.

Based on an infinitesimal element, the virtual work method yields the relation between the surface-induced traction and the surface energy density,

$$\boldsymbol{\gamma}_t = \nabla_s \phi,\ \gamma_n \boldsymbol{n} = \phi \left(\frac{1}{R_1} + \frac{1}{R_2} \right) \boldsymbol{n} = \phi \left(\boldsymbol{n} \cdot \nabla_s \right) \boldsymbol{n} \tag{2}$$

where ∇_s is a surface gradient operator, ϕ is the surface energy density in the current configuration (relative to the reference configuration as shown in Fig. 1), and R_1 and R_2 are the principal radii of curvature of a curved surface.

Using the relation between the Eulerian surface energy density ϕ in the current configuration and the Lagrangian surface energy density ϕ_0 in the reference configuration,

$$\phi = \frac{\phi_0}{J_s}, \tag{3}$$

yields the final equilibrium equation and boundary condition,

$$\begin{cases} \boldsymbol{\sigma} \cdot \nabla + \boldsymbol{f} = 0 \,(\text{in} V - S) \\ \boldsymbol{n} \cdot \boldsymbol{\sigma} \cdot \boldsymbol{n} = \boldsymbol{p} \cdot \boldsymbol{n} - \phi_0 \left(\boldsymbol{n} \cdot \nabla_s \right) / J_s \,(\text{on } S) \\ (\boldsymbol{I} - \boldsymbol{n} \otimes \boldsymbol{n}) \cdot \boldsymbol{\sigma} \cdot \boldsymbol{n} = (\boldsymbol{I} - \boldsymbol{n} \otimes \boldsymbol{n}) \cdot \boldsymbol{p} + \phi_0 \left(\nabla_s J_s \right) / J_s^2 - \nabla_s \phi_0 / J_s \,(\text{on } S) \end{cases} \tag{4}$$

where J_s is a Jacobian determinant characterizing the surface deformation from the reference configuration to the current one. Equation (3) can also be found in Nix and Gao [37] and Huang and Wang [38].

The Lagrangian surface energy density ϕ_0 in the reference configuration can be further divided into a structural part ϕ_0^{stru} and a chemical part ϕ_0^{chem}. The former is related to the surface strain energy induced by the surface relaxation and the external loading, while the latter originates from the surface dangling-bond energy, i.e.,

$$\begin{aligned} \phi_0 &= \phi_0^{\text{stru}} + \phi_0^{\text{chem}}, \\ \phi_0^{\text{stru}} &= \frac{E_b}{2 \sin \beta} \sum_{i=1}^{2} a_{0i} \eta_i \left\{ \begin{array}{l} \left[3 + \left(\lambda_i + \lambda_i \varepsilon_{si} \right)^{-m} - 3 \left(\lambda_i + \lambda_i \varepsilon_{si} \right) \right] \times \\ \left[\lambda_i^2 \varepsilon_{si}^2 + \left(\lambda_i - 1 \right)^2 + 2 \lambda_i \left(\lambda_i - 1 \right) \varepsilon_{si} \right] \end{array} \right\}, \\ \phi_0^{\text{chem}} &= \phi_{0b} \left(1 - \frac{D_0}{w_1 D} \right), \eta_1 = a_{01} / a_{02},\ \eta_2 = a_{02} / a_{01} \end{aligned} \tag{5}$$

where ϕ_{0b} is the bulk surface energy density, D_0 is a critical size ($D_0 = 3d_a$ for nanoparticles, nanowires, and $2d_a$ for nano-films, where d_a is the atomic diameter). D is a characteristic scale of nanomaterials (e.g., thickness and diameter). w_1 is a parameter governing the size-dependent behavior of ϕ_0^{chem}. E_b is the bulk Young's modulus. a_{01}, a_{02} represent the initial lattice lengths in the two principal directions on surface,

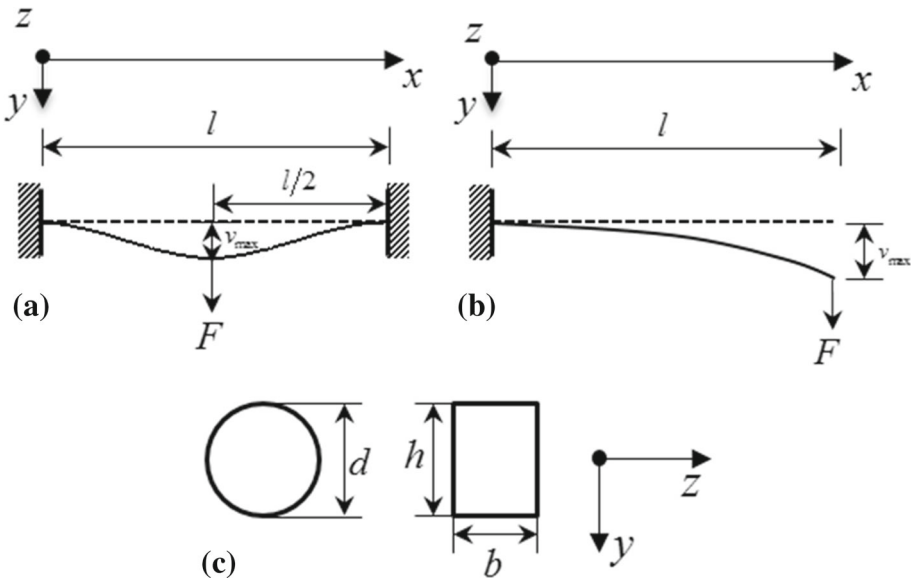

Fig. 2 Bending model of a nanobeam with a global coordinate system (x, y, z). **a** A fixed–fixed nanobeam with a concentrated force acting at the middle of the nanobeam; **b** a cantilevered nanobeam with a concentrated force acting at the free end; **c** cross sections of the two kinds of nanobeams

respectively, as shown in Fig. 1. After spontaneous surface relaxation, the lattice lengths become a_{r1} and a_{r2}, and further become a_1 and a_2 in the current configuration when subjected to an external loading. $\lambda_i = a_{ri}/a_{0i}$ denotes the surface relaxation parameter; $\varepsilon_{si} = (a_i - a_{ri})/a_{ri}$ is the surface strain induced only by the external loading; m is a parameter describing the dependence of bond lengths on the binding energy ($m = 4$ for alloys or compounds and $m = 1$ for pure metals). Detailed derivations of Eq. (5) can be found in the reference of Chen and Yao [32].

As shown by Eqs. (4) and (5), the surface effect of a nano-solid can be characterized by two independent parameters, i.e., the surface energy density of bulk materials and the surface relaxation parameter, both of which have clearly physical meanings and are very easy to determine by experiment and simple MD simulation.

3 Surface effect in a Timoshenko nanobeam

As shown in Fig. 2, the length of a nanobeam in the x direction is l, and the vertical deflection in the y direction is v. The cross section of the nanobeam can be rectangular with a height h and a width b ($b \geq h$), or circular with a diameter d. Based on the new elastic theory, the static bending behavior of the nanobeam with two kinds of boundary conditions will be investigated, i.e., a fixed–fixed beam and a cantilevered one. The shear deformation effect is included in all the analyses.

3.1 The potential energy function of a bending Timoshenko nanobeam

The shear deformation effect on the beam's deflection is taken into account in this paper. The deflection slope $\mathrm{d}v/\mathrm{d}x$ of the bending nanobeam can be decomposed into two parts, i.e., the rotation angle θ of the cross section only due to pure bending and the additional slope α caused by shear deformation [39],

$$\frac{\mathrm{d}v}{\mathrm{d}x} = \theta + \alpha, \tag{6}$$

The axial and vertical displacements u_x, u_y, and the axial strain ε_x are expressed as

$$u_x = -y\theta, \quad u_y = v, \quad \varepsilon_x = -\frac{\mathrm{d}\theta}{\mathrm{d}x}y. \tag{7}$$

Then, the bending moment M and the shear force V can be obtained,

$$M = -E_b I_z \frac{\mathrm{d}\theta}{\mathrm{d}x}, \quad V = kG_b A\alpha = kG_b A\left(\frac{\mathrm{d}v}{\mathrm{d}x} - \theta\right) \tag{8}$$

where E_b is the bulk Young's modulus (Young's modulus of bulk materials), $G_b = E_b/[2(1+\nu)]$ is the bulk shear modulus, and ν is the bulk Poisson's ratio. $I_z = \int_A y^2 \mathrm{d}A$ represents the inertia moment of the cross section, A is the area of the cross section, and k denotes a shear coefficient depending on the shape of cross section, where $k = 5(1+\nu)/(6+5\nu)$ for a rectangular cross section and $k = 6(1+\nu)/(7+12\nu+4\nu^2)$ for a circular one.

Combining Eqs. (6)–(8) yields the variation of bulk strain energy,

$$\begin{aligned}\delta U &= -\int_0^l M\delta\left(\frac{\mathrm{d}\theta}{\mathrm{d}x}\right)\mathrm{d}x + \int_0^l V\delta\left(\frac{\mathrm{d}v}{\mathrm{d}x} - \theta\right)\mathrm{d}x \\ &= -\int_0^l \left[E_b I_z \frac{\mathrm{d}^2\theta}{\mathrm{d}x^2} + kG_b A\left(\frac{\mathrm{d}v}{\mathrm{d}x} - \theta\right)\right]\delta\theta\mathrm{d}x - \int_0^l kG_b A\left(\frac{\mathrm{d}^2 v}{\mathrm{d}x^2} - \frac{\mathrm{d}\theta}{\mathrm{d}x}\right)\delta v\mathrm{d}x \\ &\quad + \left[E_b I_z \frac{\mathrm{d}\theta}{\mathrm{d}x}\delta\theta\right]_0^l + \left[kG_b A\left(\frac{\mathrm{d}v}{\mathrm{d}x} - \theta\right)\delta v\right]_0^l.\end{aligned} \tag{9}$$

The variation of surface energy can be written as

$$\delta\Phi = \int_{S_{nw}} \boldsymbol{\gamma}\cdot\delta\boldsymbol{u}\mathrm{d}S = \int_0^l \mathrm{d}x \int_{C_{nw}} (\gamma_x\delta u_x + \gamma_n\delta u_n)\,\mathrm{d}C \tag{10}$$

where S_{nw} represents the lateral surface of nanobeams, C_{nw} is the perimeter of a rectangular or circular cross section, $\delta u_x = -y\delta\theta$ and $\delta u_n \approx \delta v$ are the tangential and normal displacement components of $\delta\boldsymbol{u}$, respectively. γ_x and γ_n represent the tangential and normal components of surface-induced traction, which, according to Eq. (2), can be formulated in terms of the Lagrangian surface energy density,

$$\begin{cases}\gamma_x = \dfrac{\mathrm{d}\phi}{\mathrm{d}x} = \dfrac{\mathrm{d}}{\mathrm{d}x}\left(\dfrac{\phi_0}{J_s}\right) = \dfrac{1}{J_s}\dfrac{\mathrm{d}\phi_0}{\mathrm{d}x} - \dfrac{\phi_0}{J_s^2}\dfrac{\mathrm{d}J_s}{\mathrm{d}x} \\ \gamma_n = \phi\kappa \approx \dfrac{\mathrm{d}^2 v}{\mathrm{d}x^2}\phi = \dfrac{\phi_0}{J_s}\dfrac{\mathrm{d}^2 v}{\mathrm{d}x^2}\end{cases} \tag{11}$$

where the curvature $\kappa = -(\boldsymbol{n}\cdot\nabla_s) = \mathrm{d}^2 v/\mathrm{d}x^2$.

Similar to the existing literatures [18–21], a [100] axially oriented nanobeam with a symmetric lateral surface is considered for simplicity, which has an equal atom spacing in both bond directions, e.g., the (001) or (010) surface. The lateral surface of a circular nanobeam, which may consist of different crystal facets [6,40], is assumed as a perfectly and isotropically cylindrical surface in the theoretical analysis [18,21,26]. Thus, the Lagrangian surface energy density of such a nanobeam can be expressed as [33–35],

$$\begin{aligned}\phi_0 = \phi_{0b}\left(1 - \frac{3d_a}{4D}\right) + \frac{\sqrt{2}E_b a_0}{2}\left[3 + \frac{1}{\lambda\,(1+\varepsilon_x/2)} - 3\left(\lambda + \frac{\lambda\varepsilon_x}{2}\right)\right] \\ \left[\frac{\lambda^2\varepsilon_x^2}{4} + 2\lambda\,(\lambda-1)\,\frac{\varepsilon_x}{2} + (\lambda-1)^2\right]\end{aligned} \tag{12}$$

where λ denotes the surface relaxation parameter in both bond directions of (001) surface, a_0 denotes the bulk lattice constant. D can be taken as the diameter or height of nanobeams.

Combining Eqs. (11) and (12) and noting $J_s = \lambda^2\,(1+\varepsilon_x/2)^2$, the axial surface-induced traction γ_x can be finally written as

$$\gamma_x = \frac{1}{J_s}\frac{\mathrm{d}\phi_0}{\mathrm{d}x} - \frac{\phi_0}{J_s^2}\frac{\mathrm{d}J_s}{\mathrm{d}x} = \left[C_0 y + C_1 y^2\frac{\mathrm{d}\theta}{\mathrm{d}x} + C_2 y^3\left(\frac{\mathrm{d}\theta}{\mathrm{d}x}\right)^2\right]\frac{\mathrm{d}^2\theta}{\mathrm{d}x^2},$$

$$C_0 = \phi_0^*\,(5-4\lambda) - \frac{\sqrt{2}E_b a_0 A_2\,(3-2\lambda)}{2},$$

$$C_1 = 2\phi_0^* + \sqrt{2}E_b a_0 A_1\,(3-2\lambda) - \sqrt{2}E_b a_0 A_2\,(3-2\lambda),$$

$$
\begin{aligned}
C_2 &= \frac{\sqrt{2}E_b a_0 A_1 (7-4\lambda)}{2} - \sqrt{2}E_b a_0 A_2,\\
\phi_0^* &= \phi_{0b}\left(1-\frac{3d_a}{4D}\right) + \frac{\sqrt{2}E_b a_0}{2}(\lambda-1)^2,\\
A_1 &= \frac{1-10(\lambda-1)-17(\lambda-1)^2}{4}, A_2 = (\lambda-1)-5(\lambda-1)^2,
\end{aligned} \tag{13}
$$

and the normal surface-induced traction γ_n can be expressed as

$$
\begin{aligned}
\gamma_n &= \frac{\phi_0}{J_s}\frac{\mathrm{d}^2 v}{\mathrm{d}x^2} = \left[D_0 + D_1 y\frac{\mathrm{d}\theta}{\mathrm{d}x} + D_2 y^2\left(\frac{\mathrm{d}\theta}{\mathrm{d}x}\right)^2\right]\frac{\mathrm{d}^2 v}{\mathrm{d}x^2},\\
D_0 &= \phi_0^*(3-2\lambda), D_1 = \phi_0^* - \frac{\sqrt{2}E_b a_0 A_2 (3-2\lambda)}{2},\\
D_2 &= \frac{\sqrt{2}E_b a_0 A_1 (3-2\lambda) - \sqrt{2}E_b a_0 A_2}{2}.
\end{aligned} \tag{14}
$$

Then, Eq. (10) becomes

$$
\delta\Phi = -\int_0^l \left\{\left[C_0 I_{S1} + C_2 I_{S2}\left(\frac{\mathrm{d}\theta}{\mathrm{d}x}\right)^2\right]\frac{\mathrm{d}^2\theta}{\mathrm{d}x^2}\delta\theta + \left[D_0 I_{C1} + D_2 I_{S1}\left(\frac{\mathrm{d}\theta}{\mathrm{d}x}\right)^2\right]\frac{\mathrm{d}^2 v}{\mathrm{d}x^2}\delta v\right\}\mathrm{d}x \tag{15}
$$

in which $I_{S1} = \int_{C_{NW}} y^2 \mathrm{d}C$, $I_{S2} = \int_{C_{NW}} y^4 \mathrm{d}C$, $I_{C1} = -\int_{C_{nw}} n_w^2 \mathrm{d}C$. Here, n_w represents the vertical component of the unit normal vector n, which is parallel to v. For the cross section of different shapes, we have

$$
\begin{aligned}
\text{Rectangular: } I_z &= \frac{bh^3}{12}, \quad I_{S1} = \frac{bh^2}{2} + \frac{h^3}{6}, \quad I_{S2} = \frac{bh^4}{8} + \frac{h^5}{40}, \quad I_{C1} = 2b, A = bh\\
\text{Circular: } I_z &= \frac{\pi d^4}{64}, \quad I_{S1} = \frac{\pi d^3}{8}, \quad I_{S2} = \frac{3\pi d^5}{128}, \quad I_{C1} = \frac{\pi d}{2}, \quad A = \frac{\pi d^2}{4}
\end{aligned} \tag{16}
$$

where the height h of a rectangular cross section and the diameter d of a circular one possess a nanometer scale.

Combining Eqs. (9) and (15) leads to the variation of the potential energy function,

$$
\begin{aligned}
\delta\Pi &= \delta U + \delta\Phi - \delta W\\
&= -\int_0^l \left[\left(E_b I_z + C_0 I_{S1}\right)\frac{\mathrm{d}^2\theta}{\mathrm{d}x^2} + kG_b A\left(\frac{\mathrm{d}v}{\mathrm{d}x} - \theta\right)\right]\delta\theta\mathrm{d}x\\
&\quad -\int_0^l \left[\left(kG_b A + D_0 I_{C1}\right)\frac{\mathrm{d}^2 v}{\mathrm{d}x^2} - kG_b A\frac{\mathrm{d}\theta}{\mathrm{d}x}\right]\delta v\mathrm{d}x\\
&\quad + \left[E_b I_z\frac{\mathrm{d}\theta}{\mathrm{d}x}\delta\theta\right]_0^l + \left[kG_b A\left(\frac{\mathrm{d}v}{\mathrm{d}x} - \theta\right)\delta v\right]_0^l - F\delta v_{\max}.
\end{aligned} \tag{17}
$$

3.2 Closed-form solution of a fixed–fixed Timoshenko nanobeam

A fixed–fixed nanobeam is shown in Fig. 2a, where two ends $x = 0$ and $x = l$ are clamped and a concentrated force F is applied at $x = l/2$. The maximum deflection at $x = l/2$ is denoted as $v_{\max}$. Due to the symmetry of the structure, only half of the nanobeam is considered. The variation of the potential energy in Eq. (17) can be rewritten as

$$\begin{aligned}\delta\Pi = &-\int_0^{l/2}\left[\left(E_bI_z + C_0I_{S1}\right)\frac{\mathrm{d}^2\theta}{\mathrm{d}x^2} + kG_bA\left(\frac{\mathrm{d}v}{\mathrm{d}x} - \theta\right)\right]\delta\theta\mathrm{d}x \\ &-\int_0^{l/2}\left[\left(kG_bA + D_0I_{C1}\right)\frac{\mathrm{d}^2v}{\mathrm{d}x^2} - kG_bA\frac{\mathrm{d}\theta}{\mathrm{d}x}\right]\delta v\mathrm{d}x \\ &+\left[E_bI_z\frac{\mathrm{d}\theta}{\mathrm{d}x}\delta\theta\right]_0^{l/2} + \left[kG_bA\left(\frac{\mathrm{d}v}{\mathrm{d}x} - \theta\right)\delta v\right]_0^{l/2} - \frac{F}{2}\left(\delta v\right)_{x=l/2}. \end{aligned} \tag{18}$$

Let $\delta\Pi = 0$, $x = l\hat{x}$, $v(x) = l\hat{v}\left(\hat{x}\right)$, and $\theta(x) = \hat{\theta}\left(\hat{x}\right)$. The normalized equilibrium equations and the boundary conditions can be written as

$$\begin{cases}\left(1+\chi_1\right)\chi_3\frac{\mathrm{d}^2\hat{\theta}}{\mathrm{d}\hat{x}^2} + \left(\frac{\mathrm{d}\hat{v}}{\mathrm{d}\hat{x}} - \hat{\theta}\right) = 0 \\ \left(1+\chi_2\chi_3\right)\frac{\mathrm{d}^2\hat{v}}{\mathrm{d}\hat{x}^2} - \frac{\mathrm{d}\hat{\theta}}{\mathrm{d}\hat{x}} = 0\end{cases} \tag{19}$$

$$\begin{cases}\left(\frac{\mathrm{d}\hat{v}}{\mathrm{d}\hat{x}} - \hat{\theta}\right)_{\hat{x}=1/2} = \chi_3\chi_4 \\ \hat{v}(0) = 0 \\ \hat{\theta}(0) = 0 \\ \hat{\theta}(1/2) = 0\end{cases} \tag{20}$$

where $\chi_1 = C_0I_{S1}/(E_bI_z)$, $\chi_2 = D_0I_{C1}l^2/(E_bI_z)$, $\chi_3 = E_bI_z/\left(kG_bAl^2\right)$, and $\chi_4 = Fl^2/(2E_bI_z)$. Among them, χ_1 and χ_2 are two dimensionless parameters characterizing the surface effect. When the characteristic size of a beam is large enough, χ_1 and χ_2 tend to zero. Then, Eq. (19) can be reduced to the classical Timoshenko beam theory,

$$\begin{cases}\chi_3\frac{\mathrm{d}^2\hat{\theta}}{\mathrm{d}\hat{x}^2} + \left(\frac{\mathrm{d}\hat{v}}{\mathrm{d}\hat{x}} - \hat{\theta}\right) = 0 \\ \frac{\mathrm{d}^2\hat{v}}{\mathrm{d}\hat{x}^2} - \frac{\mathrm{d}\hat{\theta}}{\mathrm{d}\hat{x}} = 0\end{cases}. \tag{21}$$

Solving Eq. (19) with boundary conditions in Eq. (20) yields the closed-form solution of the deflection,

$$\begin{aligned}\hat{v}\left(\hat{x}\right) = &\frac{\chi_4\left(1+\chi_2\chi_3\right)}{\chi_2}\hat{x} + \frac{\chi_4}{\xi\chi_2\cosh\left(\xi/4\right)}\sinh\left[\xi\left(1/4 - \hat{x}\right)\right] \\ &-\frac{\chi_4\tanh\left(\xi/4\right)}{\xi\chi_2}\left(0 < \hat{x} < 1/2\right)\end{aligned} \tag{22}$$

with the maximum deflection $\hat{v}_{\max}$ at $\hat{x} = 1/2$,

$$\hat{v}_{\max}\left(\hat{x}\right) = \hat{v}(1/2) = \frac{\chi_4\left(1+\chi_2\chi_3\right)}{2\chi_2} - \frac{2\chi_4\tanh\left(\xi/4\right)}{\xi\chi_2} \tag{23}$$

where $\xi = \sqrt{\chi_2/[(1+\chi_1)(1+\chi_2\chi_3)]}$.

For a nanobeam with a relatively large aspect ratio, the shear deformation can be neglected, i.e., $\chi_3 = 0$. Then, Eq. (22) can be well degraded to the deflection of a fixed–fixed Euler–Bernoulli nanobeam [33].

Equating Eq. (23) with the classical Euler beam solution

$$\hat{v}_{\max}^{E_c} = \hat{v}^{E_c}(1/2) = \frac{Fl^3}{192E_bI_z} = \frac{\chi_4}{96} \tag{24}$$

leads to the effective elastic modulus of a fixed–fixed Timoshenko nanobeam E_{eff},

$$\frac{E_{\mathrm{eff}}}{E_b} = \frac{\chi_2\xi}{48\left[\left(1+\chi_2\chi_3\right)\xi - 4\tanh\left(\xi/4\right)\right]}. \tag{25}$$

Without considering the shear deformation and surface effects, i.e., $\chi_3 = 0$, $\chi_1 \to 0$ and $\chi_2 \to 0$, Eq. (25) can be well reduced to 1.

3.3 Closed-form solution of a cantilevered Timoshenko nanobeam

For a cantilevered Timoshenko nanobeam as shown in Fig. 2b, the fixed end is at $x = 0$, and a concentrated force F is applied at the other end $x = l$. The variation of the potential energy can be written as

$$\begin{aligned}\delta\Pi &= \delta U + \delta\Phi - \delta W \\ &= -\int_0^l \left[\left(E_b I_z + C_0 I_{S1}\right)\frac{\mathrm{d}^2\theta}{\mathrm{d}x^2} + kG_bA\left(\frac{\mathrm{d}v}{\mathrm{d}x} - \theta\right)\right]\delta\theta\,\mathrm{d}x \\ &\quad -\int_0^l \left[\left(kG_bA + D_0 I_{C1}\right)\frac{\mathrm{d}^2 v}{\mathrm{d}x^2} - kG_bA\frac{\mathrm{d}\theta}{\mathrm{d}x}\right]\delta v\,\mathrm{d}x \\ &\quad + \left[E_b I_z\frac{\mathrm{d}\theta}{\mathrm{d}x}\delta\theta\right]_0^l + \left[kG_bA\left(\frac{\mathrm{d}v}{\mathrm{d}x} - \theta\right)\delta v\right]_0^l - F\left(\delta v\right)_{x=l}. \end{aligned} \tag{26}$$

Let $\delta\Pi = 0$. The achieved equilibrium equation has the same form as that in Eq. (19), and the boundary condition for a cantilevered Timoshenko nanobeam can be written as

$$\begin{cases} \left(\frac{\mathrm{d}\hat{v}}{\mathrm{d}\hat{x}} - \hat{\theta}\right)_{\hat{x}=1} = 2\chi_3\chi_4 \\ \hat{v}\left(0\right) = 0 \\ \hat{\theta}\left(0\right) = 0 \\ \frac{\mathrm{d}\hat{\theta}(1)}{\mathrm{d}\hat{x}} = 0 \end{cases}. \tag{27}$$

Solving Eq. (19) with the boundary conditions in Eq. (27) yields the closed-form solution of the deflection of a cantilevered Timoshenko nanowire,

$$\begin{aligned}\hat{v}\left(\hat{x}\right) &= \frac{2\chi_4\left(1+\chi_2\chi_3\right)}{\chi_2}\cosh\left(\xi\right)\hat{x} + \frac{2\chi_4}{\xi\chi_2}\sinh\left[\xi\left(1-\hat{x}\right)\right] \\ &\quad -\frac{2\chi_4\sinh\left(\xi\right)}{\xi\chi_2}\left(0 < \hat{x} < 1\right)\end{aligned} \tag{28}$$

with the maximum deflection $\hat{v}_{\max}$ at $\hat{x} = 1$,

$$\hat{v}_{\max}\left(\hat{x}\right) = \hat{v}\left(1\right) = \frac{2\chi_4\left(1+\chi_2\chi_3\right)}{\chi_2}\cosh\left(\xi\right) - \frac{2\chi_4\sinh\left(\xi\right)}{\xi\chi_2}. \tag{29}$$

Equating Eq. (29) with the classical solution

$$\hat{v}_{\max}^{E_c} = \hat{v}^{E_c}\left(1\right) = \frac{Fl^2}{3E_bI_z} = \frac{2}{3}\chi_4 \tag{30}$$

leads to the effective elastic modulus of a cantilevered nanobeam,

$$\frac{E_{\mathrm{eff}}}{E_b} = \frac{\chi_2\xi}{3\left[\left(1+\chi_2\chi_3\right)\xi\cosh\left(\xi\right) - \sinh\left(\xi\right)\right]}. \tag{31}$$

Without considering the shear deformation and surface effects, i.e., $\chi_3 = 0$, $\chi_1 \to 0$ and $\chi_2 \to 0$, the effective elastic modulus can be well reduced to the bulk value E_b.

4 Results and discussion

The surface and shear deformation effect on the static bending behavior of a Timoshenko nanobeam are analyzed in this Section. As a typical example, we consider silver and silicon nanobeams with (100) lateral surfaces. The isotropic surface relaxation parameter λ can be empirically expressed as $\lambda = 1 - c_r/D$ ($c_r > 0$, $D = h$ or d) [41–43]. When the characteristic size D is large enough ($D \geq 5$ nm), λ tends to be unity. Values of c_r and the other material parameters involved in our model are listed in Table 1 [11,44,45].

Table 1 Material parameters involved in our model [44–46]

	d_a (nm)	a_0 (nm)	E_b (GPa)	ν	$\phi_{0b(001)}$ (N/m)	$c_{1(001)}$ (nm)	τ_0 (N/m)	E_s (N/m)
Ag	0.2889	0.418	78	0.37	1.2	0.016	0.89	1.22
Si	0.22	0.54	169	0.25	2.2	/	/	/

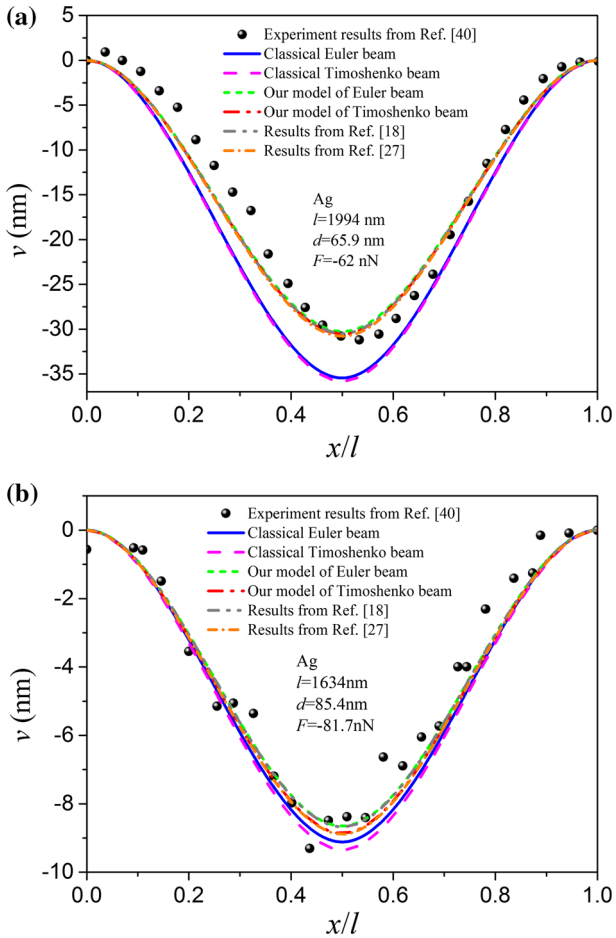

Fig. 3 Deflection of a silver nanobeam with a fixed–fixed boundary, where theoretical predictions of different elastic theories with or without surface effect are compared with the existing experimental results. **a** For a nanobeam with the length $l = 1994\,\text{nm}$, the diameter $d = 65.9\,\text{nm}$ and the concentrated force $F = -62\,\text{nN}$. **b** For a nanobeam with the length $l = 1634\,\text{nm}$, the diameter $d = 85.4\,\text{nm}$ and the concentrated force $F = -81.7nN$

4.1 The case of a fixed–fixed nanobeam

The deflection of a fixed–fixed Timoshenko silver (Ag) nanobeam is theoretically predicted as shown in Fig. 3 and compared with the existing experimental measurement [40], where the result of an Euler–Bernoulli nanobeam achieved by the same elastic theory [33] is also given for comparison, as well as the results obtained by the surface elasticity model [18,27] and the classical elasticity theory [39] for Euler–Bernoulli and Timoshenko beams. All the material parameters are taken from the experiment work [40]. $l = 1994\,\text{nm}, d = 65.9\,\text{nm}$, $F = -62\,\text{nN}$ in Fig. 3a, and $l = 1634\,\text{nm}$, $d = 85.4\,\text{nm}$, $F = -81.7$ nN in Fig. 3b. The involved surface elastic modulus E_s in the surface elasticity model is taken as 1.22 N/m [18].

From Fig. 3, one can see that all the theoretical results considering the surface effect agree well with the experimental ones, while the classical one deviate from the experimental measurement, especially the maximum deflection. Both the theoretical predictions and the experimental data demonstrate that the bending stiffness of a fixed–fixed nanobeam can be effectively enhanced due to the surface effect. It is also found that the deflections predicted by the Euler–Bernoulli and Timoshenko theories with the surface effect, respectively,

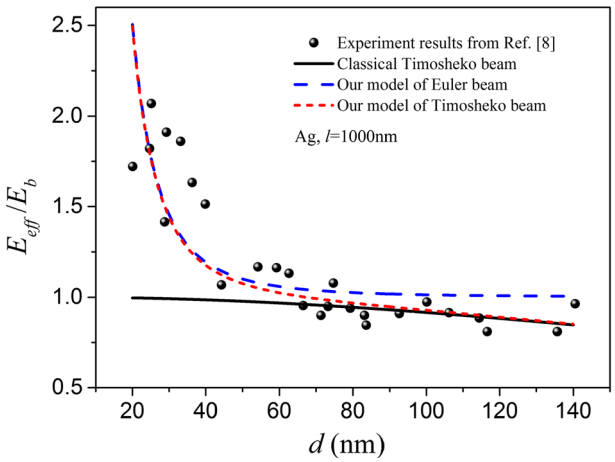

Fig. 4 Normalized effective elastic modulus given by an existing experiment measurement or predicted by different elastic models as a function of the diameter of a fixed–fixed silver nanobeam

almost coincide with each other since the aspect ratio of the nanobeam is relatively large (about 30) in Fig. 3a. However, a noticeable difference between the Euler–Bernoulli and Timoshenko predictions for the nanobeam in Fig. 3b can be found, which is due to a relatively small aspect ratio (about 19) in this case. Such a result demonstrates that the shear deformation effect on the bending behavior of nanobeams becomes more significant with a reducing aspect ratio, which is also consistent with the macroscopic beam case.

The difference of the results with and without considering the shear deformation effect can be further found in Fig. 4, where the normalized effective elastic modulus of a silver nanobeam varies with the diameter of the circular nanobeam but with a fixed beam length $l = 1000$ nm. Experimental result and that predicted by the classical Timoshenko beam theory are also given for comparison [8]. It is clearly shown that the normalized effective elastic modulus E_{eff} decreases significantly with the increase in the nanobeam diameter not only for the Euler–Bernoulli result with surface effect but also for the Timoshenko one with surface effect. Both results agree with the experimental measurement [8]. However, when the diameter is relatively small, less than 40 nm in this case, both the Euler–Bernoulli result and the Timoshenko one with surface effect agree well with each other but deviate significantly from the classical Timoshenko result, which denotes that only the surface effect is obvious and the shear deformation effect can be neglected for nanobeams with a relatively large aspect ratio but with a small diameter, $l/d \geq 25$ in this case. As the diameter is larger than 40 nm but less than 90 nm, the Timoshenko result including the surface effect deviates obviously from the Euler–Bernoulli one as well as the classical Timoshenko result, which demonstrates that not only the surface effect but also the shear deformation one should be considered for nanobeams with an intermediate aspect ratio as well as an intermediate diameter. However, when the diameter is further larger than 90 nm, both the Timoshenko result including surface effect and the classical Timoshenko one are consistent well with each other as well as the experimental measurement [8], but the Euler–Bernoulli result with surface effect deviates obviously from them. It denotes that the surface effect can be neglected but the shear deformation effect should be included for nanobeams with a relatively large diameter but with a small aspect ratio. Each theoretical result agrees well with the experimental ones at each adaptive region as shown in Fig. 4. Comparing the Euler–Bernoulli result with the Timoshenko one yields that the shear deformation could decrease the effective stiffness of a stubby beam. In contrast to the bulk Young's modulus, the effective Young's modulus predicted by the Timoshenko theory with surface effect is reduced when the aspect ratio is relatively small, which also demonstrates a negative effect of shear deformation on the overall stiffness. However, when the aspect ratio becomes large, the effective Young's modulus predicted by the Timoshenko theory with surface effect could be larger than the bulk one. Such a result leads to an interesting fact that a fixed–fixed nanobeam with an increasing aspect ratio would experience a transition from softening to stiffening due to competition between the surface effect and the shear deformation effect.

4.2 The case of a cantilevered nanobeam

Experimental measurement of the effective elastic modulus for a silicon cantilevered nanobeam with a rectangular cross section has been carried out by Sadeghian et al. [11], where the width of the nanobeam is

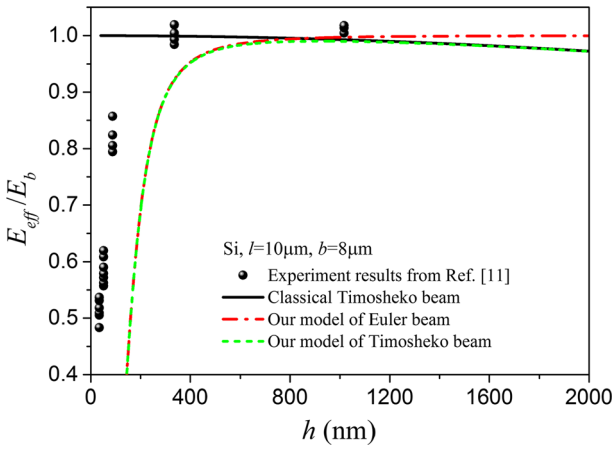

Fig. 5 Normalized effective elastic modulus given by an existing experiment measurement or predicted by different elastic models as a function of the height of a rectangular silicon cantilevered nanobeam

$b = 8\mu$m, the axial length is $l = 10\mu$m, and the height h varies from 40 nm to 2μm. Theoretical predictions of the effective elastic modulus by both the Euler–Bernoulli and Timoshenko theories are given in Fig. 5, where the classical Timoshenko result and the experimental one are exhibited for comparison. It is obvious that the cantilevered nanobeam shows a softening behavior in contrast to the stiffening one of a fixed–fixed nanobeam when the characteristic length decreases, the height of the nanobeam in this case. Such a softening behavior of a cantilevered nanobeam has also been observed in many other studies [10,11,23,46]. The deflection curvature of a cantilevered nanobeam under a concentrated force at the free end should be responsible for the softening behavior, which leads to the component of the surface-induced traction with the same direction as that of the external load. In contrast, the component of the surface-induced traction in most parts of a fixed–fixed bending nanobeam has an opposite direction to that of the external load, acting as a resistance to the external load, which consequently leads to the stiffening behavior of a fixed–fixed nanobeam [18,33]. Comparing the theoretical results with the experimental one as shown in Fig. 5 shows that surface effect would dominate when the characteristic length of a cantilevered nanobeam is relatively small (a relatively small height corresponding to a relatively large aspect ratio, since the axial length l is fixed), while the shear deformation effect would play a dominant role when the aspect ratio is relatively small (a relatively large height corresponding to a relatively large characteristic length, since the axial length l is fixed). The competition mechanism of the surface effect and the shear deformation one is much similar to that for a fixed–fixed nanobeam except the softening and stiffening phenomenon. It should be noted that all the effective elastic moduli in the present paper are achieved by equating the maximum deflection considering surface effect with the one of a classical Euler–Bernoulli beam, consistent also with the experimental work [11]. Therefore, in the case with a large enough height, only the normalized result of an Euler beam will approach to 1, while the normalized result of a Timoshenko beam cannot approach to 1 but to the normalized classical solution of a Timoshenko beam as shown in Fig. 5.

From Fig. 5, one can see that an obvious difference between the theoretical result and the experimental one exists for the silicon nanobeam, especially at the small height region, though the varying trend of the effective elastic modulus predicted theoretically is consistent with that measured experimentally. A few aspects may be responsible for such a deviation. $m = 1$ is adopted for silicon materials in the theoretical prediction, but such a value is more appropriate for a pure metal. The beam bending theory is used to analyze samples in the experiment, which look more like a plate than a beam. Moreover, as mentioned by Sadeghian et al. [11], the fabrication-induced defects and the native oxide layer within nanobeam samples may also have important influences on the experimental measurements of stiffness, which, however, are not considered in the present model.

5 Conclusions

The static bending behavior of nanobeams with different boundary conditions is investigated using the new elastic theory for nanomaterials [32] and considering the shear deformation effect. Closed-form solutions of the deflection and effective elastic modulus for nanobeams are obtained. A comparison has been carried out

among the Euler–Bernoulli beam solution with surface effect, the Timoshenko beam solution with surface effect, and the classical beam solution. It is found that the surface effect will dominate for both a fixed–fixed Timoshenko nanobeam and a cantilevered one when the characteristic length is relatively small, while the shear deformation effect will play a key role and the surface effect can be omitted when the characteristic length is relatively large. Both the surface effect and the shear deformation one should be included when the characteristic length is intermediate. The present result would provide a comprehensive understanding of which effect should be included when predicting the bending behavior of a nanobeam as well as the stiffening and softening mechanisms of a nanobeam. It should be useful for the design of nanobeam-based devices with desired precision measurements.

Acknowledgements The work reported here is supported by NSFC through Grants #11532013, #11372317, #11402270 and the CAS/SAFEA International Partnership Program for Creative Research Teams.

References

1. Rogers, J.A., Someya, T., Huang, Y.G.: Materials and mechanics for stretchable electronics. Science **327**, 1603–1607 (2010)
2. Cui, Y., Wei, Q.Q., Park, H., Lieber, C.M.: Nanowire nanosensors for highly sensitive and selective detection of biological and chemical species. Science **293**, 1289–1292 (2001)
3. Xie, P., Xiong, Q.H., Fang, Y., Qing, Q., Lieber, C.M.: Local electrical potential detection of DNA by nanowire-nanopore sensors. Nat. Nanotechnol. **7**, 119–125 (2012)
4. Gong, C., Liang, J., Hu, W., Niu, X., Ma, S., Hahn, H.T., Pei, Q.: A healable, semitransparent silver nanowire-polymer composite conductor. Adv. Mater. **25**, 4186–4191 (2013)
5. Liang, H., Upmanyu, M., Huang, H.: Size-dependent elasticity of nanowires: nonlinear effects. Phys. Rev. B **71**, 241403 (2005)
6. Cuenot, S., Frétigny, C., Demoustier-Champagne, S., Nysten, B.: Surface tension effect on the mechanical properties of nanomaterials measured by atomic force microscopy. Phys. Rev. B **69**, 165410 (2004)
7. Chen, T.Y., Chiu, M.S., Weng, C.N.: Derivation of the generalized Young-Laplace equation of curved interfaces in nanoscaled solids. J. Appl. Phys. **100**, 074308 (2006)
8. Jing, G.Y., Duan, H.L., Sun, X.M., Zhang, Z.S., Xu, J., Li, Y.D., Wang, J.X., Yu, D.P.: Surface effects on elastic properties of silver nanowires: contact atomic-force microscopy. Phys. Rev. B **73**, 235409 (2006)
9. Nam, C.Y., Jaroenapibal, P., Tham, D., Luzzi, D.E., Evoy, S., Fischer, J.E.: Diameter-dependent electromechanical properties of GaN nanowires. Nano Lett. **6**, 153–158 (2006)
10. Gavan, K.B., Westra, H.J., van der Drift, E.W., Venstra, W.J., van der Zant, H.S.: Size-dependent effective Young's modulus of silicon nitride cantilevers. Appl. Phys. Lett. **94**, 233108 (2009)
11. Sadeghian, H., Yang, C.K., Goosen, J.F., Bossche, A., Staufer, U., French, P.J., van Keulen, F.: Effects of size and defects on the elasticity of silicon nanocantilevers. J. Micromech. Microeng. **20**, 064012 (2010)
12. Celik, E., Guven, I., Madenci, E.: Mechanical characterization of nickel nanowires by using a customized atomic force microscope. Nanotechnology **22**, 155702 (2011)
13. Gurtin, M.E., Murdoch, A.I.: A continuum theory of elastic material surfaces. Arch. Ration. Mech. Anal. **57**, 291–323 (1975)
14. Gurtin, M.E., Murdoch, A.I.: Surface stress in solids. Int. J. Solids Struct. **14**, 431–440 (1978)
15. Dingreville, R., Qu, J., Cherkaoui, M.: Surface free energy and its effect on the elastic behavior of nano-sized particles, wires and films. J. Mech. Phys. Solids **53**, 1827–1854 (2005)
16. Duan, H.L., Wang, J., Huang, Z.P., Karihaloo, B.L.: Size-dependent effective elastic constants of solids containing nano-inhomogeneities with interface stress. J. Mech. Phys. Solids **53**, 1574–1596 (2005)
17. Wang, G.F., Feng, X.Q.: Effects of surface elasticity and residual surface tension on the natural frequency of microbeams. Appl. Phys. Lett. **90**, 231904 (2007)
18. He, J., Lilley, C.M.: Surface effect on the elastic behavior of static bending nanowires. Nano Lett. **8**, 1798–1802 (2008)
19. Chhapadia, P., Mohammadi, P., Sharma, P.: Curvature-dependent surface energy and implications for nanostructures. J. Mech. Phys. Solids **59**, 2103–2115 (2011)
20. Chiu, M.S., Chen, T.: Effects of high-order surface stress on static bending behavior of nanowires. Phys. E **44**, 714–718 (2011)
21. Song, F., Huang, G., Park, H., Liu, X.: A continuum model for the mechanical behavior of nanowires including surface and surface-induced initial stresses. Int. J. Solids Struct. **48**, 2154–2163 (2011)
22. Liu, J., Mei, Y., Xia, R., Zhu, W.: Large displacement of a static bending nanowire with surface effects. Phys. E **44**, 2050–2055 (2012)
23. Park, S., Kim, J., Park, J., Lee, J., Choi, Y., Kwon, O.: Molecular dynamics study on size-dependent elastic properties of silicon nanocantilevers. Thin Solid Films **492**, 285–289 (2005)
24. Mohammadi, P., Sharma, P.: Atomistic elucidation of the effect of surface roughness on curvature-dependent surface energy, surface stress, and elasticity. Appl. Phys. Lett. **100**, 133110 (2012)
25. Georgakaki, D., Ziogos, O., Polatoglou, H.: Vibrational and mechanical properties of Si/Ge nanowires as resonators: a molecular dynamics study. Phys. Status Solidi Appl. Mater. **211**, 267–276 (2014)
26. Wang, G.F., Feng, X.Q.: Timoshenko beam model for buckling and vibration of nanowires with surface effects. J. Phys. D: Appl. Phys. **42**, 155411 (2009)
27. Jiang, L.Y., Yan, Z.: Timoshenko beam model for static bending of nanowires with surface effects. Phys. E **42**, 2274–2279 (2010)

28. Li, X.F., Zhang, H., Lee, K.Y.: Dependence of Young's modulus of nanowires on surface effect. Int. J. Mech. Sci. **81**, 120–125 (2014)
29. Miller, R.E., Shenoy, V.B.: Size-dependent elastic properties of nanosized structural elements. Nanotechnology **11**, 139 (2000)
30. Shenoy, V.B.: Atomistic calculations of elastic properties of metallic fcc crystal surfaces. Phys. Rev. B **71**, 094104 (2005)
31. Mi, C., Jun, S., Kouris, D.A., Kim, S.Y.: Atomistic calculations of interface elastic properties in noncoherent metallic bilayers. Phys. Rev. B **77**, 075425 (2008)
32. Chen, S.H., Yao, Y.: Elastic theory of nanomaterials based on surface-energy density. J. Appl. Mech. **81**, 121002 (2014)
33. Yao, Y., Chen, S.H.: Surface effect in the bending of nanowires. Mech. Mater. **100**, 12–21 (2016)
34. Yao, Y., Chen, S.H.: Surface effect on resonant properties of nanowires predicted by an elastic theory for nanomaterials. J. Appl. Phys. **118**, 044303 (2015)
35. Yao, Y., Chen, S.: Buckling behavior of nanowires predicted by a new surface energy density model. Acta Mech. **227**, 1799–1811 (2016)
36. Huang, Z.P., Sun, L.: Size-dependent effective properties of a heterogeneous material with interface energy effect: from finite deformation theory to infinitesimal strain analysis. Acta Mech. **190**, 151–163 (2007)
37. Nix, W.D., Gao, H.J.: An atomistic interpretation of interface stress. Scr. Mater. **39**, 1653–1661 (1998)
38. Huang, Z.P., Wang, J.: A theory of hyperelasticity of multi-phase media with surface/interface energy effect. Acta Mech. **182**, 195–210 (2006)
39. Timoshenko, S.P., Goodier, J.N.: Theory of Elasticity, 3rd edn. McGraw-Hill, New York (1970)
40. Chen, Y., Dorgan Jr., B.L., Mcllroy, D.N., Aston, D.E.: On the importance of boundary conditions on nanomechanical bending behavior and elastic modulus determination of silver nanowires. J. Appl. Phys. **100**, 104301 (2006)
41. Diao, J., Gall, K., Dunn, M.L.: Atomistic simulation of the structure and elastic properties of gold nanowires. J. Mech. Phys. Solids **52**, 1935–1962 (2004)
42. Ouyang, G., Li, X., Tan, X., Yang, G.: Surface energy of nanowires. Nanotechnology **19**, 045709 (2008)
43. Olsson, P.A., Park, H.S.: On the importance of surface elastic contributions to the flexural rigidity of nanowires. J. Mech. Phys. Solids **60**, 2064–2083 (2012)
44. Jaccodine, R.: Surface energy of germanium and silicon. J. Electrochem. Soc. **110**, 524–527 (1963)
45. Sheng, H., Kramer, M., Cadien, A., Fujita, T., Chen, M.: Highly optimized embedded-atom-method potentials for fourteen fcc metals. Phys. Rev. B **83**, 134118 (2011)
46. Moshtaghin, A.F., Naghdabadi, R., Asghari, M.: Effects of surface residual stress and surface elasticity on the overall yield surfaces of nanoporous materials with cylindrical nanovoids. Mech. Mater. **51**, 74–87 (2012)